Chapter 3

Functional analysis of a zebrafish *myd88* mutant identifies key transcriptional components of the innate immune system

Michiel van der Vaart, Joost J. van Soest, Herman P. Spaink,

and Annemarie H. Meijer

Disease models & mechanisms 6, 2013

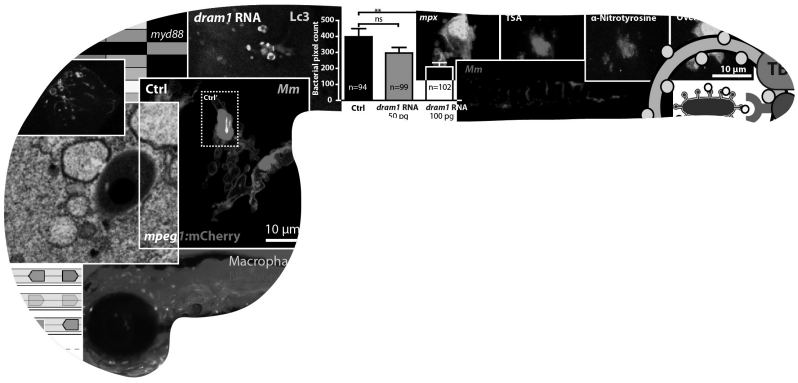

Abstract

Toll-like receptors (TLRs) are an important class of pattern recognition receptors (PRRs) that recognize microbial and danger signals. Their downstream signaling upon ligand-binding is vital for initiation of the innate immune response. In human and mammalian models, myeloid differentiation factor 88 (MYD88) is known for its central role as an adaptor molecule in interleukin 1 receptor (IL-1R) and TLR-signalling. The zebrafish is increasingly used as a complementary model system for disease research and drug screening. Here, we describe a line with a truncated version of Myd88 as the first zebrafish mutant for a TLR-signaling component. We show that this immune-compromised mutant has a lower survival rate under standard rearing conditions and is more susceptible to challenge with the acute bacterial pathogens *Edwardsiella tarda* and *Salmonella typhimurium*. Microarray and quantitative PCR (qPCR) analysis revealed that expression of genes for transcription factors central to innate immunity, including NFκB and AP-1, and the pro-inflammatory cytokine Ill1b, is dependent on Myd88-signalling during these bacterial infections. Nevertheless, expression of immune genes independent of Myd88 in the *myd88* mutant line was sufficient to limit growth of an attenuated *S. typhimurium* strain. In the case of infection with the chronic bacterial pathogen *Mycobacterium marinum*, we show that Myd88-signaling has an important protective role during early pathogenesis. During mycobacterial infection, the *myd88* mutant shows accelerated formation of granuloma-like aggregates and increased bacterial burden, with associated lower induction of genes central to innate immunity. This zebrafish *myd88* mutant will be a valuable tool to further study the role of IL1R- and TLR-signaling in innate immunity processes underlying infectious diseases, inflammatory disorders, and cancer.

Introduction

The host innate immune response is the first line of defense against invading microbes. Its function is to recognize invading pathogens at the first stage of infection and initiate an appropriate immune response[1]. Pathogen-associated molecular patterns (PAMPs) and damage-associated molecular patterns (DAMPs) are recognized by pattern recognition receptors (PRRs), of which the Toll-like receptor (TLR) family has been studied most extensively[1, 2]. Myeloid differentiation factor 88 (MYD88) is an important adaptor protein in the TLR signaling pathway, since it is used by all TLRs except for TLR3 [3]. Its C-terminal TIR-domain enables interaction with TLRs, while the N-terminal death domain enables interaction with IL-1 receptor associated kinase 4 (IRAK4), which in turn recruits IRAK1 or IRAK2 to form the 'Myddosome' signalling complex, activating NF-κB (nuclear factor κB) and MAP-kinase (mitogen activated protein) signaling[4-8]. The Myddosome also functions downstream of the receptors for interleukin 1 (IL-1), IL-18 and IL-33, and it has been associated with IFN-Y receptor signaling, adding to its central role in inflammation and host defense[5, 9, 10].

Patients with a deficiency in MYD88 suffer from a primary immunodeficiency syndrome[11, 12]. This syndrome is characterized by an increased susceptibility to pyogenic bacteria, like *Streptococcus pneumonia*, *Staphylococcus aureus*, *Pseudomonas aeruginosa* and *Salmonella* species[13]. Mice deficient in Myd88 were shown to be hyporesponsive to lipopolysaccharide (LPS) Il-1 stimulation and resistant to endotoxic shock[9, 14, 15]. As a consequence of their reduced ability to recognize PAMPs, Myd88-deficient mice are more susceptible to infection by *Toxoplasma gondii* parasites[16] and several bacterial pathogens, including *S. aureus*[17], *Listeria monocytogenes*[18], *Chlamydia pneumonia*[19], and *Mycobacterium tuberculosis*[20].

The zebrafish (*Danio rerio*) is an excellent model to study the innate immune system that can complement research in mouse models and human cell lines[21]. Major advantages are its suitability for genetic approaches, high-throughput screening, and live imaging studies that make use of the many available fluorophore-marked transgenic lines. As early as one day post fertilization (dpf), zebrafish embryos are capable of mounting an effective innate immune response against microbial infections[22]. This immune response has a transcriptional signature similar to responses observed in mammalian and cell culture systems[23]. Furthermore, the major PRRs, their downstream signaling pathways, and innate effector mechanisms are conserved between humans and zebrafish[24]. Expression of *myd88* in zebrafish leukocytes was confirmed using a transgenic reporter line[25]. Maturation of the adaptive immune system is not complete until approximately three weeks post fertilization[26], providing a window of at least two weeks in which the innate immunity can be studied in the absence of T- and B-cell responses.

The use of zebrafish as a model for infectious diseases, inflammatory disorders, cancer, and other immune related diseases is growing rapidly[27]. Therefore, zebrafish mutants for important components of the immune system are eagerly awaited. As an alternative to mutant lines, morpholino antisense oligonucleotides may be used for blocking of protein production, but knockdown by morpholinos is only temporal and may also cause off-target effects[28]. Knockdown of Myd88 by morpholino in zebrafish embryos affected their ability to combat infection with the attenuated *Salmonella enterica* serovar *Typhimurium* (*S. typhimurium*) Ra strain[29]. It was also shown that expression of the pro-inflammatory cytokine gene *il1b* was dependent on Myd88, both during Salmonella infection and when embryos were stimulated with TLR ligands[23, 30]. Knockdown analysis also demonstrated a role for Myd88 in LPS- or trinitrobenzene sulfonic acid (TNBS)-induced intestinal inflammation and microbial-dependent intestinal epithelial cell proliferation in zebrafish larvae[31-33].

Here we characterize the first *myd88* mutant zebrafish line (*myd88*$^{-/-}$) and compare its immune response to that of wild types when infected with the bacterial pathogens *Edwardsiella tarda*, *Salmonella typhimurium*, and *Mycobacterium marinum*. The mutant allele contains a premature stopcodon, resulting in a truncated protein that lacks part of its death domain and the complete TIR-domain, required for interaction

with IRAK4 and TLRs respectively. As expected, the homozygous mutant showed an immune compromised phenotype. We show that *myd88*$^{-/-}$ zebrafish embryos are more susceptible to infection by all three pathogens tested, but have sufficient remaining innate immunity to limit infection with attenuated *S. typhimurium* Ra bacteria. Finally, we compare the gene expression profile of *myd88*$^{-/-}$ embryos with that of wild type embryos to distinguish between Myd88-dependent and -independent gene expression upon infection with different pathogens. This analysis revealed that gene expression of transcription factors central to innate immunity, including NFκB and AP-1, and many innate immunity signalling and effector genes is dependent on Myd88-signalling during bacterial infections. Using this mutant as a model for mycobacterial pathogenesis, we demonstrated that Myd88-signaling has an important protective role during early stages of tuberculosis.

Results

Reduced survival of homozygous *myd88* mutants

Sequencing of an ENU-mutagenized zebrafish library resulted in the identification of a *myd88* mutant allele, *myd88*^{hu3568}, which carries a T to A point mutation creating a premature stopcodon (figure 1A). The mutation is located in the N-terminal death domain, leading to a truncated protein, lacking part of its death domain required for interaction with Irak4. The truncated protein is also missing the complete C-terminal TIR-domain required for interaction with the cytoplasmic TIR-domain of TLRs. In addition, we observed that the mutant transcript is less stable than the wild type transcript (supplementary figure 1). Zebrafish embryos homozygous for the mutation were found at Mendelian frequencies after crossing of heterozygous parents. They showed no developmental differences with their wild type siblings and could only be distinguished by genotyping. Two groups of *myd88*$^{-/-}$ and *myd88*$^{+/+}$ embryos were compared under normal embryo rearing conditions to test for differences in unchallenged survival during development. Up to 8 dpf there was no difference in survival between mutants and wild types (figure 1B). After this period *myd88*$^{-/-}$ larvae showed a significantly decreased survival rate compared to wild type larvae (figure 1B). The steady decline of *myd88*$^{-/-}$ larvae ceased at around 20 dpf. Thus, under our rearing conditions, 8 – 20 dpf was a critical period for rearing *myd88*$^{-/-}$ larvae, but subsequent development was normal and adults were capable of breeding. We have experienced that the success rate of rearing *myd88*$^{-/-}$ families is highly variable. Furthermore, *myd88*$^{-/-}$ adults display an increased mortality rate compared to wild type individuals and heterozygotes, often showing pathological features linked with infection (data not shown). To conclude, we observe a reduced survival in embryonic and adult *myd88*$^{-/-}$ zebrafish, most likely caused by a primary immune deficiency due to the lack of functional Myd88.

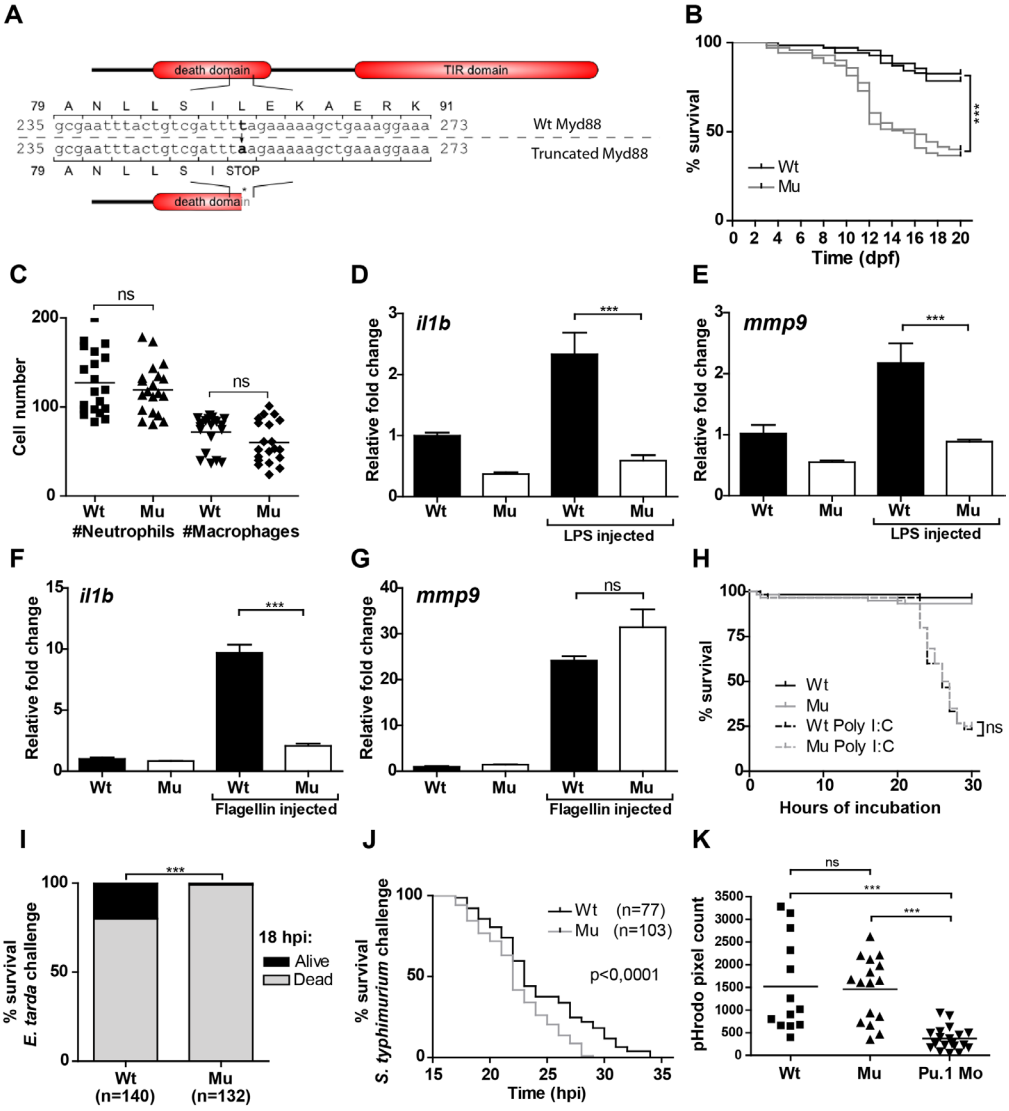

Figure 1. Characterization of *myd88* mutant zebrafish and survival following infection with *E. tarda* and S. *typhimurium*. (A) Mutant sequence and protein structure. A point mutation (T to A) in the death domain sequence of zebrafish *myd88* introduces a premature stopcodon. The truncated protein lacks the TIR domain and part of the death domain. Nucleotide and amino acid positions are indicated with respect to the translation start codon (B). Survival assays. Percentage survival during the first 20 days of development (under unchallenged conditions) is shown for two groups (n=70 per group) of *myd88*$^{-/-}$ mutants (Mu, grey lines) and *myd88*$^{+/+}$ wild type (Wt, black lines), grown in two individual experiments. The groups are the F1 offspring of *myd88*$^{-/-}$ and *myd88*$^{+/+}$ siblings born from heterozygous parents. At 20 dpf, 83% and 79% of wild types survived, compared to 37% and 40% of mutants. The asterisks indicate the significant difference between wild type and mutant survival (p<0.0001), tested with a logrank test. (C). Quantification of leukocyte numbers. Total numbers of GFP-labeled neutrophils in 3 dpf *myd88*$^{-/-}$-*mpx*::*egfp* and *myd88*$^{+/+}$-*mpx*::*egfp* embryos (n=20 per group) were counted under a

fluorescence stereo microscope. Total numbers of macrophages were determined by performing whole mount L-plastin immunohistochemistry and deducting the number of *mpx::egfp*-positive neutrophils from the number of L-plastin-positive total leukocytes per embryo. Each data point represents an individual embryo and lines indicate the mean value. No significant difference (ns) in numbers of neutrophils or macrophages was observed with a t-test. (D-G). *Myd88*$^{-/-}$ and wild type embryos were injected with purified LPS (100 µg/ml), flagellin (100 µg/ml), or PBS as a control. Expression of *il1b* and *mmp9* at 2 hours post injection was analyzed by qPCR. Data are combined from three biological replicates (n=20 per group) and statistical significance was determined by one-way ANOVA with Tukey's Multiple Comparison method as a post-hoc test (***, p<0.001 and **, p<0.01). (H). Poly I:C exposure. *Myd88*$^{-/-}$ and wild type embryos were exposed to poly I:C (500 µg/ml eggwater) starting at 5 dpf. Survival curves are based on data pooled from two individual experiments (n=60 per group in total). Statistical significance (ns) was determined by a logrank test. (I) *E. tarda* infection. At 28 hpf, *myd88*$^{-/-}$ and wild type embryos were infected with approximately 150 CFU *E. tarda* FL6-60 by injection into the blood island. The percentages of embryos surviving infection at 18 hpi are shown for *myd88*$^{-/-}$ (Mu, n=132, 1% surviving) and wild type (Wt, n=140, 20% surviving). Data is pooled from two individual experiments and statistical significance (***, p<0.001) was tested with a contingency test. (J) *S. typhimurium* infection. Embryos were injected into the blood island at 28 hpf with approximately 150 CFU of *S. typhimurium* strain SL1027. Survival curves for mutant (n=103, median survival 22 hpi) and wild type embryos (n=77, median survival 23 hpi) are based on data pooled from two individual experiments. Statistical significance (p<0.001) was determined by a logrank test. (K) Phagocytosis assay. Mutant and wild type embryos were injected at 28 hpf into the blood island with *E. coli* cell wall particles labeled with a pH-dependent fluorogenic dye, pHrodo. After 2 hours, stereo fluorescence images were taken for fluorescent pixel quantification. Pu.1 morpholino-injected embryos (Pu.1 Mo), deficient in phagocytic leukocytes, were included as a control. Each data point represents an individual embryo and lines indicate the mean value. No significant difference (ns) was observed between wild type and mutant embryos, but both groups were significantly different (***, p<0.001) from Pu.1 morpholino-injected controls by one-way ANOVA with Tukey's Multiple Comparison method as a post-hoc test .

Myd88 deficiency has no overt effect on leukocyte development

To test whether *myd88*$^{-/-}$ embryos have normal leukocyte development, we crossed *myd88*$^{-/-}$ adults with fish carrying the *mpx::egfp* transgene that specifically marks neutrophils[34]. Leukocyte differentiation was assessed at 3 dpf by GFP fluorescence of neutrophils in combination with fluorescent immunohistochemistry for the pan-leukocytic marker L-plastin (leukocyte-plastin). We observed no differences between mutant and wild type larvae in the total numbers of the two major subtypes of leukocytes, neutrophils (*mpx*::GFP/L-plastin double fluorescent cells) and macrophages (L-plastin positive and *mpx*::GFP negative) (figure 1C). Therefore, we conclude that early leukocyte hematopoiesis in zebrafish embryos is not overtly affected by Myd88 deficiency and does not account for the reduced survival observed when rearing *myd88*$^{-/-}$ families.

Myd88-dependent signaling is required for recognition of LPS and flagellin, but not Poly I:C

It is expected that *myd88*$^{-/-}$ embryos are affected in their ability to sense and respond to microbial PAMPs. To test this hypothesis, we injected LPS purified from *S. typhimurium*

into the blood island of 28 hpf *myd88*$^{-/-}$ and wild type embryos. We isolated RNA 2 hours post injection (hpi) and determined the response to LPS by analyzing the expression of *il1b* and *mmp9* by quantitative PCR (qPCR). It has been reported that, unlike in humans, recognition of LPS in fish does not occur via Tlr4[35, 36]. Nevertheless, we show here that recognition of LPS in zebrafish embryos does require Myd88, since expression of both *il1b* and *mmp9* after injection with LPS was significantly lower in mutants compared to wild types (figure 1D, E). We also injected groups of embryos with flagellin, a known ligand for the Tlr5-Myd88 pathway in zebrafish[23]. The observed expression levels of *il1b* following injection confirmed the Myd88-dependency for flagellin recognition (fig 1F). Interestingly, flagellin-induced *mmp9* expression occurred independent of Myd88. As a negative control, we also tested poly I:C, a ligand of Tlr3, the only TLR that is known to signal completely independent of MyD88. Poly I:C injection did not lead to a reproducible induction of immune related genes in 1 dpf embryos (data not shown). We therefore determined the sensitivity to poly I:C exposure by incubation starting at 5 dpf. We observed a sharp decrease in survival after approximately 24 hours of incubation, which was similar between *myd88*$^{-/-}$ and wild type embryos, showing that poly I:C recognition and toxicity occurs Myd88-independently, in contrast to the MyD88-dependent recognition of LPS and flagellin.

Increased susceptibility of *myd88*$^{-/-}$ embryos to acute bacterial pathogens is not caused by a general defect in phagocytosis

To test the ability of *myd88*$^{-/-}$ embryos to mount a successful defense response, we infected 28 hpf *myd88*$^{-/-}$ and wild type embryos by blood island injection with two acute bacterial pathogens: *E. tarda* and *S. typhimurium*. These two pathogens are known to cause progressive and fatal infection in wild type zebrafish embryos[37, 38]. At 18 hpi with *E. tarda*, the percentage of surviving *myd88*$^{-/-}$ embryos (1%) was significantly lower than the percentage of wild type embryos (20%) that had not yet succumbed to the infection (figure 1I). Lethality of *S. typhimurium* infection also occurred significantly faster in mutant than in wild type embryos (figure 1J). These results demonstrate that *myd88*$^{-/-}$ embryos are affected in their response towards invading pathogens. To exclude the possibility that the impaired immune response might be due to a defect in phagocytosis of bacteria in *myd88*$^{-/-}$ embryos, we injected both mutants and wild types with *Escherichia coli* cell wall particles labelled with the pH-dependent fluorogenic dye, pHrodo. This provides a quantitative measure for phagocytosis, since pHrodo only becomes fluorescent in acidic environments, like those encountered in the phagolysosomal pathway[25]. The results showed similar levels of phagocytosis in *myd88*$^{-/-}$ and wild type embryos at 2 hours post injection (figure 1K). A control group, where a Pu.1 morpholino was injected to severely deplete leukocyte populations[39], showed low levels of phagocytosis. These results demonstrate that the increased susceptibility of *myd88*$^{-/-}$ embryos to acute bacterial pathogens is not the result of a defect in phagocytosing bacterial components, but that *myd88*$^{-/-}$ embryos are not capable of mounting a wild type innate immune response towards these bacteria at a stage after primary phagocytosis.

The expression of genes that function in immunity are affected in the *myd88*$^{-/-}$ mutant after infection with *E. tarda* and *S. typhimurium*

To study the effect of Myd88 deficiency on gene expression during infection, we analyzed the transcriptome profile of *myd88*$^{-/-}$ and *myd88*$^{+/+}$ embryos infected with *E. tarda* and *S. typhimurium*. Embryos from a heterozygous incross (*myd88*$^{+/-}$) were infected by injecting 150 CFU of either pathogen into the blood island at 28 hpf. Embryos injected with the carrier solution alone were taken along as a control. At 8 hpi, RNA was isolated from three *myd88*$^{-/-}$ and three wild type individuals per condition. Transcriptome analysis of uninfected *myd88*$^{-/-}$ and wild type embryos showed that no immune related genes were differentially expressed in the absence of Myd88, except for *myd88* itself, which was consistently downregulated in Myd88-deficient embryos ($p<0.00001$). Eight hours after infection with *E. tarda* or *S. typhimurium*, a large number of probes (619 and 1214, respectively) were upregulated in wild type embryos (figure 2A). In comparison, the numbers of upregulated probes were approximately 3-fold lower in *myd88*$^{-/-}$ embryos (190 for *E. tarda* and 339 for *S. typhimurium*) (figure 2A). At the same time point, the smaller number of downregulated probes was comparable between wild types (199 for *E. tarda* and 315 for *S. typhimurium*) and *myd88*$^{-/-}$ embryos (117 for *E. tarda* and 196 for *S. typhimurium*) (figure 2B). Gene ontology (GO) analysis revealed that the GO term 'Immune system process' was significantly enriched both in wild type and in *myd88*$^{-/-}$ embryos infected with *E. tarda* or *S. typhimurium* (figure 2C). However, while all GO terms belonging to the 'Immune system process' subclass were enriched for infected wild type embryos, only 1 or 3 out of 5 were significantly enriched for *myd88*$^{-/-}$ embryos infected with *E. tarda* or *S. typhimurium*, respectively. GO term-analysis of the probe sets that were up- or down- regulated by the different infections in *myd88*$^{-/-}$ mutants did not reveal a specific Myd88-independent signaling pathway that has been activated to compensate for the loss of Myd88 function.

For a more in-depth analysis of gene regulation in *myd88*$^{-/-}$ and wild type embryos infected with *E. tarda* or *S. typhimurium*, we selected all immune related genes with significantly altered expression in mutants, wild types, or both (a fold change of at least 2 with $P<0,00001$ for at least two probes). A heatmap was created to visualize the expression differences of these genes between individual embryos. In agreement with genotyping of the embryos, *myd88* itself was expressed at low levels in all *myd88*$^{-/-}$ embryos. In general, infection with either bacterial strain resulted in a large scale upregulation of immune related genes in wild type embryos, while *myd88*$^{-/-}$ embryos showed a much weaker transcriptional response (figure 3). Surprisingly, however, in one of the *myd88*$^{-/-}$ embryos infected with *S. typhimurium* the response of several of the selected genes was similar to the wild type level. The most consistent differences in gene expression between *myd88*$^{-/-}$ and wild type embryos were observed for transcription factors and genes involved in signal transduction. The number of upregulated genes in these categories was lower in *myd88*$^{-/-}$ embryos, but also the expression level of genes that did respond was lower compared to wild type. The residual induction of immune-related transcription factors in *myd88*$^{-/-}$ embryos was reflected in the number

A **Upregulated probes upon infection**

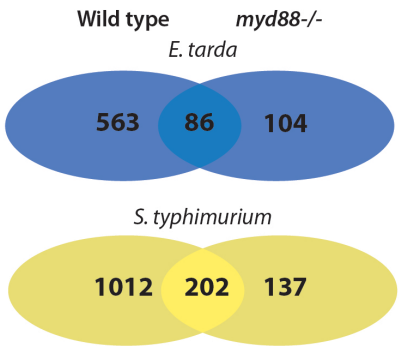

B **Downregulated probes upon infection**

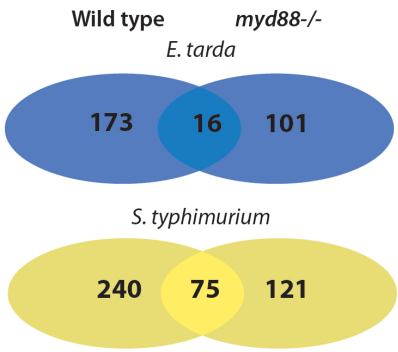

C

		Wt Et		Mu Et		Wt St		Mu St	
GO	**Name**	**#genes**	***p*-value**	**#genes**	***p*-value**	**#genes**	***p*-value**	**#genes**	***p*-value**
GO:0002376	**Immune system process**	**13**	**0.000**	**8**	**0.000**	**10**	**0.040**	**4**	**0.045**
GO:0002253	activation of immune response	2	0.002	0	1.000	2	0.011	1	0.045
GO:0002252	immune effector process	3	0.000	0	1.000	2	0.011	1	0.045
GO:0006955	immune response	13	0.000	7	0.000	8	0.009	3	0.041
GO:0002684	positive regulation of immune system process	2	0.003	0	1.000	2	0.017	1	0.055
GO:0002682	regulation of immune system process	3	0.000	0	1.000	2	0.025	1	0.066
GO:0051704	**Multi-organism process**	**12**	**0.000**	**4**	**0.000**	**11**	**0.000**	**2**	**0.048**
GO:0051707	response to other organism	12	0.000	4	0.000	11	0.000	2	0.048
GO:0050896	**Response to stimulus**	**20**	**0.000**	**9**	**0.001**	**32**	**0.000**	**11**	**0.003**
GO:0048584	positive regulation of response to stimulus	2	0.008	0	1.000	2	0.045	1	0.087
GO:0048583	regulation of response to stimulus	3	0.001	0	1.000	2	0.081	1	0.118
GO:0009607	response to biotic stimulus	12	0.000	4	0.000	11	0.000	2	0.062
GO:0009605	response to external stimulus	4	0.052	1	0.454	8	0.023	3	0.062
GO:0006950	response to stress	9	0.009	3	0.195	20	0.001	8	0.002

Figure 2. Transcriptome analysis of *myd88*$^{-/-}$ and wild type embryos following infection with *E. tarda* and *S. typhimurium*. (A,B) Venn-diagrams showing the overlap and differences between mutant (Mu) and wild type embryos in numbers of probes up-regulated (A) or down-regulated (B) by *E. tarda FL6-60* (Et) or *S. typhimurium SL1027* (St) infection. Embryos were infected with approximately 150 CFU of either pathogen into the caudal vein at 28 hpf and snap frozen individually at 8 hpi. Triplicate samples for each infection condition were compared groupwise with samples from control embryos (injected with PBS) using a common reference microarray design. Significance cut-offs for the ratios of infected vs control groups were set at 2-fold with $p < 10^{-5}$. (C) Gene ontology (GO) analysis. The table displays the enrichment of immune-related GO terms following infection of *myd88*$^{-/-}$ (Mu) and wild type (Wt) embryos with *E. tarda* (Et) or *S. typhimurium* (St). Go-term enrichment in the gene lists up-regulated by infection was determined by master-target statistical testing using eGOn (Beisvag et al., 2006) with the *Danio rerio* UniGene build #124 as background. The numbers of genes associated with each GO-term and the *p*-values for enrichment are indicated. We note that GO analysis is limited by the number of Unigene clusters annotated for zebrafish and therefore not all upregulated probes could be included in the analysis.

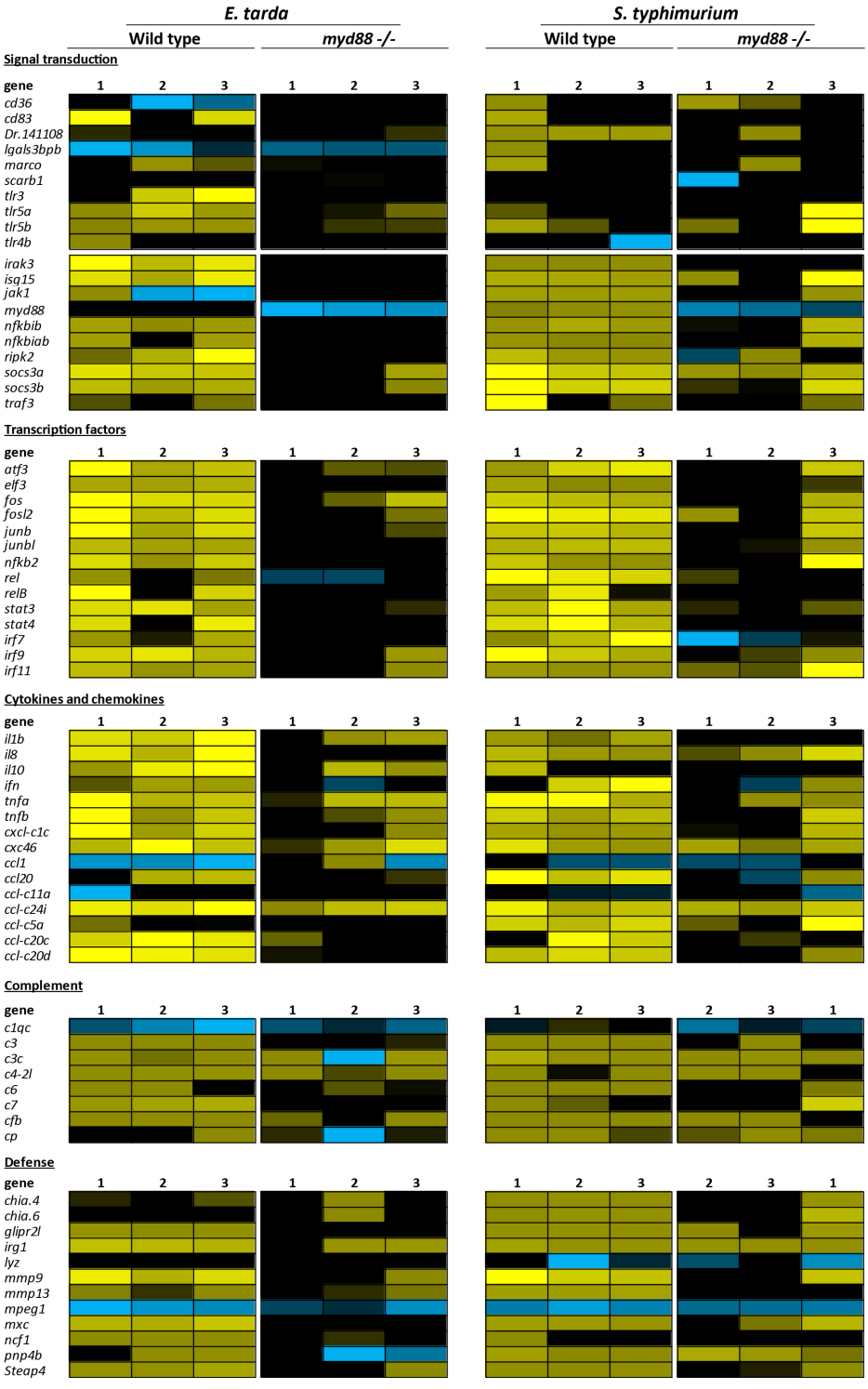
E. tarda
S. typhimurium
Wild type
myd88 -/-
Wild type
myd88 -/-
Signal transduction
gene
1 2 3 1 2 3 1 2 3 1 2 3
cd36
cd83
Dr.141108
lgals3bpb
marco
scarb1
tlr3
tlr5a
tlr5b
tlr4b
irak3
isg15
jak1
myd88
nfkbib
nfkbiab
ripk2
socs3a
socs3b
traf3
Transcription factors
gene
1 2 3 1 2 3 1 2 3 1 2 3
atf3
elf3
fos
fosl2
junb
junbl
nfkb2
rel
relB
stat3
stat4
irf7
irf9
irf11
Cytokines and chemokines
gene
1 2 3 1 2 3 1 2 3 1 2 3
il1b
il8
il10
ifn
tnfa
tnfb
cxcl-c1c
cxc46
ccl1
ccl20
ccl-c11a
ccl-c24i
ccl-c5a
ccl-c20c
ccl-c20d
Complement
gene
1 2 3 1 2 3 1 2 3 2 3 1
c1qc
c3
c3c
c4-2l
c6
c7
cfb
cp
Defense
gene
1 2 3 1 2 3 1 2 3 2 3 1
chia.4
chia.6
glipr2l
irg1
lyz
mmp9
mmp13
mpeg1
mxc
ncf1
pnp4b
Steap4

Figure 3: Comparison of the innate immune response of *myd88*$^{-/-}$ and wild type embryos to *E. tarda* and *S. typhimurium*. Gene expression profiles of *myd88*$^{-/-}$ and wild type embryos infected with *E. tarda FL6-60* or *S. typhimurium SL1027* are depicted in a heat map. Embryos were infected with 150 CFU of either pathogen into the caudal vein at 28 hpf and snap frozen individually at 8 hpi. Triplicate samples for each infection condition were compared with samples from control embryos (injected with PBS) using a common reference microarray design. Immune-related genes in the heat map are ordered in functional groups. All genes included in the heat map are represented by a minimum of two probes that showed significant up- or down-regulation (Significance cut-offs for the ratios of infected vs control groups were set at 2-fold with $p < 10^{-5}$). Up-regulation and down-regulation is indicated by increasingly bright shades of yellow and blue, respectively. All genes listed in this figure are named according to sequence homology with mammalian counterparts and in most cases have not yet been confirmed functionally.

of cytokine genes that were regulated upon infection, since those individuals that had higher expression of transcription factors also showed more significant upregulation of cytokine probes. This indicates a role for Myd88-independent signaling in the activation of these cytokine genes. Moreover, the induction of certain cytokine genes (*cxc46* and *ccl-c24i*) and components of the complement system (like *c3c*, *c4-2l*, and *cp*) did not seem to be changed in the *myd88*$^{-/-}$ embryos.

The transcription factor genes that were affected in the infected *myd88*$^{-/-}$ embryos included members of the known transcription factor families activated by TLR-MYD88 and cytokine signaling in other vertebrates: NFκB (*nfkb2*, *rel*, and *relb*), AP-1 (*fos*, *fos2l*, *junb*, and *junbl*), ATF (*atf3*) and STAT (*stat3* and *stat4*). Expression of the IRF family members, *irf7*, *irf9* and *irf11*, was dependent on Myd88 during an *E. tarda* infection, while *irf9* and *irf11* appeared Myd88-independent in the presence of *S. typhimurium*. Among the downstream cytokine genes, upregulation of *il1b* in response to *S. typhimurium* infection was strictly dependent on Myd88 in the microarray analysis. During *E. tarda* infection *il1b* was upregulated at low levels in *myd88*$^{-/-}$ embryos, with significant reduction compared to wild type embryos. The other major pro-inflammatory cytokine gene, *tnfa*, could still be upregulated in the absence of Myd88 during infections with both pathogens. Expression of the gene encoding the chemotactic cytokine Il8 was clearly dependent on Myd88 in embryos infected with *E. tarda*, while it was expressed at wild type levels in *myd88*$^{-/-}$ embryos infected with *S. typhimurium*.

In conclusion, analysis of the microarray data indicated that a large proportion of the genes which are regulated during an innate immune response against *E. tarda* or *S. typhimurium* rely on proper TLR-Myd88 or IL1R-Myd88 signaling. Without Myd88, important transcription factors, cytokines, and other genes involved in defense were upregulated at a lower level or not at all. Interestingly, we also identified genes whose upregulation was completely independent of Myd88-signaling or appeared to be pathogen specific.

Expression levels of Myd88-dependent and -independent genes are highly variable during infection

Our transcriptome analysis of *myd88*$^{-/-}$ and wild type embryos infected with *E. tarda* and *S. typhimurium* showed that Myd88-signaling is required for a large part of the gene expression involved in the innate immune response. However, performing microarray analysis on three embryos per condition revealed variation between individuals in the infection-induced expression levels of important components of the immune response. To further investigate the Myd88-dependency of a subset of these genes, we isolated RNA from a larger number (n=10) of *myd88*$^{-/-}$ and wild type embryos infected with *E. tarda* or *S. typhimurium* and performed qPCR analysis. In agreement with the microarray data, wild type embryos showed highly variable infection-induced expression levels of *il1b* (11 to 35 fold change difference compared to controls during *E. tarda* infection; 4 to 8 fold change difference in *S. typhimurium* infection) (figure 4). The *il1b* induction levels of infected *myd88*$^{-/-}$ embryos were also distributed over a broad range, but were significantly lower than in wild type embryos (2 to 20 fold change difference during *E. tarda* infection; no difference to 4 fold change difference for *S. typhimurium* infection). The expression levels of *tnfa* were spread over a similar range in wild type and *myd88*$^{-/-}$ embryos. This gene was strongly induced by *S. typhimurium* (2 to 17 fold in wild type and *myd88*$^{-/-}$), while *E. tarda* induction of *tnfa* in wild types and mutants was low and not significant. These data demonstrate that expression of *il1b* was dependent on Myd88 during infection with *E. tarda* and *S. typhimurium*, while *tnfa* expression occurred via Myd88-independent pathways during infection with *S. typhimuriu*m.

We used the same approach to analyze the expression of the matrix metalloproteinase gene *mmp9*, the chemotactic cytokine genes *il8* and *cxcl-c1c*, and the antiviral cytokine gene *ifnphi1*, in mutants and wild types infected with *E. tarda* and *S. typhimurium* (figure 4). We found that expression of *mmp9* and *cxcl-c1c* was dependent on Myd88 during infection with either pathogen, similar to *il1b*. Expression of *il8* was significantly lower in *myd88*$^{-/-}$ embryos infected with *E. tarda* compared to infected wild types. In *S. typhimurium* infection, the average induction of *il8* in *myd88*$^{-/-}$ embryos was also lower than in wild type embryos but did not result in a significant difference. Infections with *E. tarda* did not significantly induce expression levels of *ifnphi1*. Expression of *ifnphi1* was slightly upregulated in wild type embryos infected with *S. typhimurium*, but not in infected *myd88*$^{-/-}$ embryos. Interestingly, only in the case of *mmp9* expression during E. tarda infection, the induction was completely inhibited by Myd88 deficiency. All other genes that showed significant Myd88 dependency could still be induced to low levels in mutant embryos. Therefore, the important conclusion from these experiments is that pro-inflammatory gene expression in *myd88*$^{-/-}$ embryos is reduced but not completely absent.

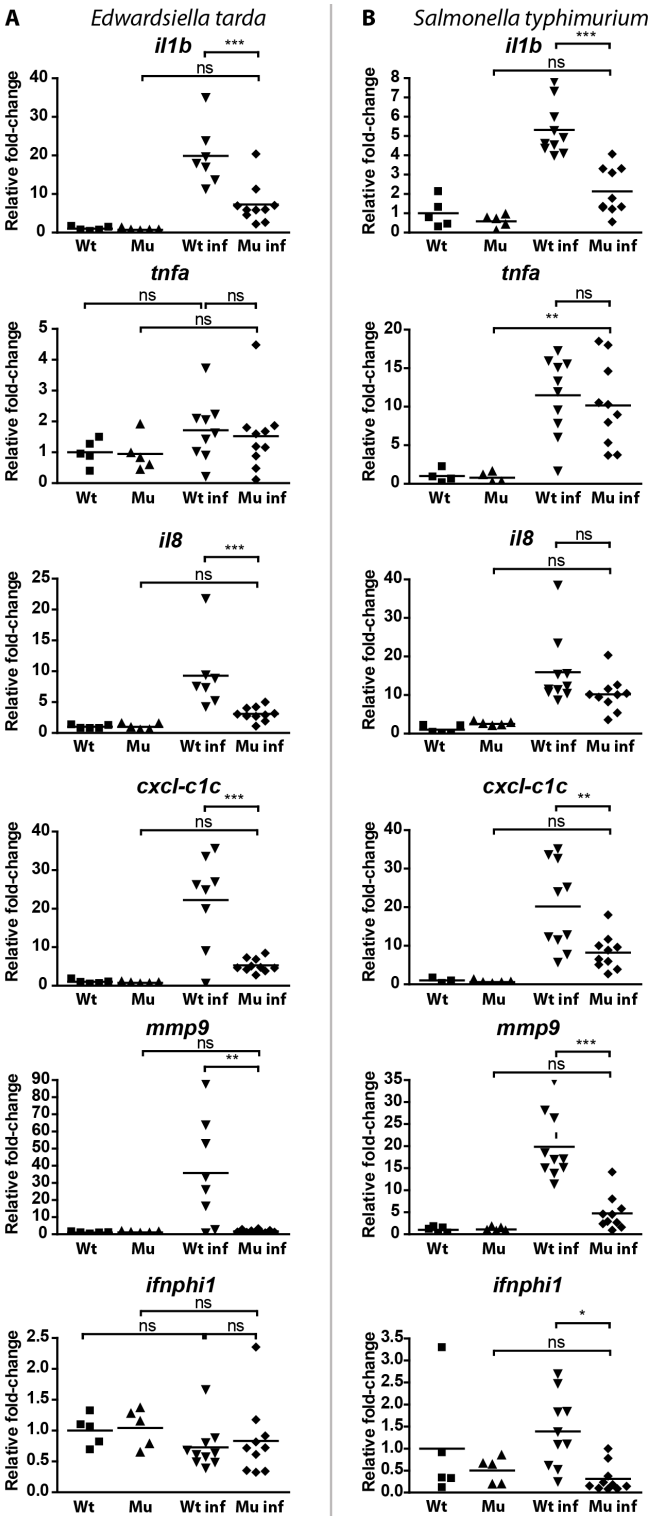

Figure 4: qPCR analysis of the response of *myd88*$^{-/-}$ and wild type embryos to *E. tarda* or *S. typhimurium* infection. Expression of *il1b*, *tnfa, il8*, *cxcl-c1c*, *mmp9*, and *ifnphi1* was analyzed by qPCR in *E. tarda* (A) or *S. typhimurium* (B) infected wild type (Wt) and mutant (Mu) embryos. RNA samples from infected embryos (inf) and uninfected controls were taken 8 hpi. Each data point represents an individual embryo and lines indicate the mean relative expression level, with uninfected wild type set at 1. Significant differences (*,p<0.05; **, p<0.01; ***, p<0.001) were calculated by one-way ANOVA with Tukey's Multiple Comparison method as a post-hoc test.

Myd88-deficient embryos can limit growth of the attenuated *S. typhimurium* Ra strain
Based on the partial induction of cytokine genes in *myd88*$^{-/-}$ embryos, we hypothesized that these embryos are not completely immune-compromised. To test this hypothesis, we infected *myd88*$^{-/-}$ and wild type embryos with a fluorescently labeled *S. typhimurium* LPS mutant (*S. typhimurium* Ra) that has previously been shown to induce attenuated infection in zebrafish embryos [38]. Four hours after injecting the bacteria into the bloodstream, we observed clustered fluorescent bacteria, indicative of phagocytosis, in both *myd88*$^{-/-}$ and wild type embryos (figure 5A and C). In contrast, clustering was greatly decreased in a Pu.1 morpholino-injected control group deficient in leukocytes (figure 5E). One day post infection, we noted increased infection in *myd88*$^{-/-}$ embryos compared to wild type, which was quantifiable by bacterial pixel counting (figure 5B, D, and G). At the same timepoint, embryos in the Pu.1 morpholino-injected control group were completely overgrown with infection, with the bacteria spreading throughout the entire vasculature (figure 5F). The bacterial pixel count in both *myd88*$^{-/-}$ and wild type embryos gradually declined over the next four days. At the 5dpi timepoint, 58% of the wild types had already cleared the infection, while wild types with remaining infection showed greatly decreased numbers of bacteria (figure 5H). At the same time, we observed a broad range of infection states in *myd88*$^{-/-}$ embryos, varying from complete clearance of the bacteria (28%) to highly infected (30%), and lethally infected (4%). Thus, embryos developed more severe infection levels under conditions of Myd88 deficiency, but still were capable of limiting the growth of the attenuated *S. typhimurium* strain. In one of the two experimental repeats, we isolated RNA from all individual infected embryos for qPCR analysis. Although *il1b* expression was lower in *myd88*$^{-/-}$ embryos compared to wild type, the difference was not significant (figure 5I). Induction of *mmp9* was also lower in *myd88*$^{-/-}$ and significantly different from the wild type embryos (figure 5J). Together, these data confirm the partial induction of pro-inflammatory genes in *myd88*$^{-/-}$ embryos and show that growth of attenuated *S. typhimurium* Ra bacteria in zebrafish embryos can be limited in a Myd88-independent manner.

***Myd88*$^{-/-}$ embryos are more susceptible to chronic infection by *Mycobacterium marinum* strains**
In contrast to the acute infections with *E. tarda* and *S. typhimurium*, *M. marinum* injection into the blood island at 28 hpf leads to a chronic infection that persists during larval development in granuloma-like aggregates of immune cells[40]. *M. marinum* is a natural pathogen of teleost fish and a close relative of *M. tuberculosis*, the causative agent of tuberculosis in humans. We aimed to address the importance of TLR-signaling during mycobacterial disease by infecting *myd88*$^{-/-}$ and wild type embryos with two different *M. marinum* strains: Mma20 and E11. Bacterial pixel counting was performed at 3 dpi for embryos infected with *M. marinum* Mma20 and at 5 dpi for embryos infected with the less virulent E11 strain. The formation of granuloma-like structures and bacterial burden in *myd88*$^{-/-}$ embryos infected with either *M. marinum* strain far exceeded that of wild types (figure 6G and H). Furthermore, we compared the effect of the *myd88* mutant during mycobacterial infection to that of a previously described

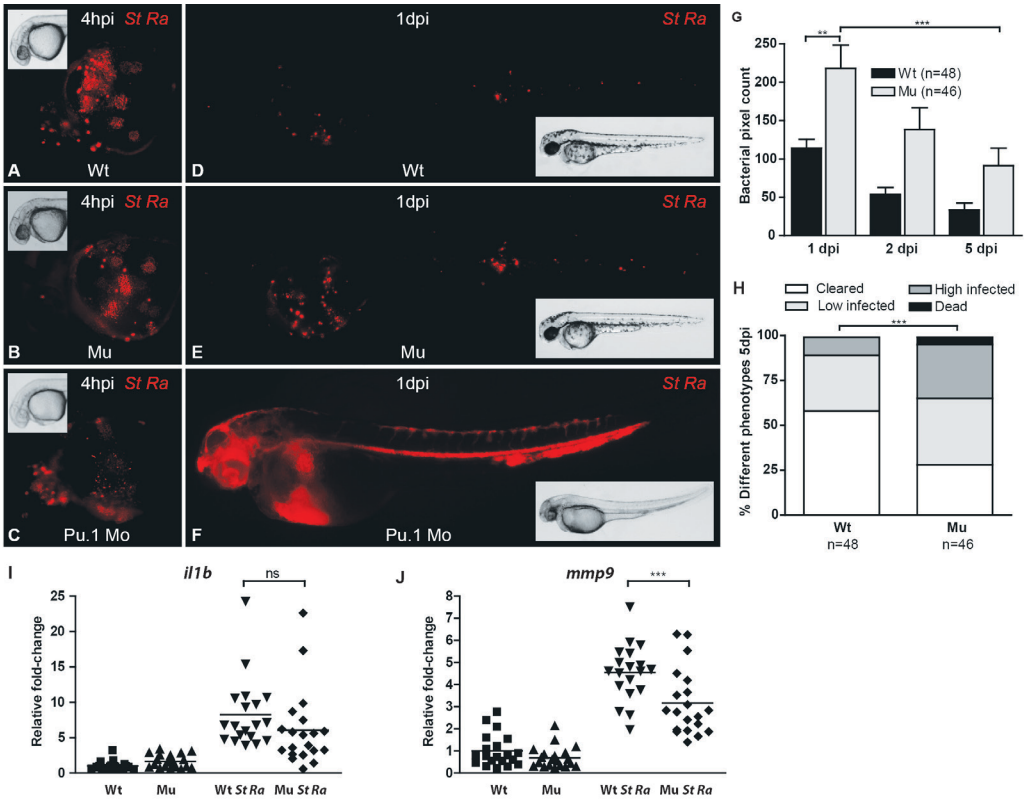

Figure 5: Bacterial burdens and qPCR analysis of gene expression in *myd88*$^{-/-}$ and wild type embryos infected with the attenuated *S. typhimurium* Ra strain. (A-F) Representative stereo fluorescence images of infected embryos. At 28 hpf, embryos were infected by injection into the blood island using approximately 150 CFU of DsRed-labeled *Salmonella typhimurium* Ra. Pu.1 morpholino-injected embryos (Pu.1 Mo: C,F), deficient in phagocytic leukocytes, were included for comparison with wild type (Wt: A,D) and *myd88*$^{-/-}$ (Mu: B,E) embryos. Dispersal of infected leukocytes over the yolk sac at 4 hpi (A-C) and the progression of infection is shown at 1 dpi (D-F). (G). Quantification of bacterial burden. Stereo fluorescence images of infected embryos at 1, 2, and 5 dpi were used for quantification of bacterial fluorescent pixels. Data is accumulated from two individual experiments. Significant differences of (**, p<0.01; ***, p<0.001) were determined by one-way ANOVA with Tukey's Multiple Comparison method as a post-hoc test. (H) Variation in phenotypes at 5 dpi. Embryos were categorized according to infection levels as cleared (no remaining bacterial fluorescent pixels or pixel count below 10), low infected (pixel count between 10 and 100), high infected (pixel count above 100), or dead. The distribution over categories was significantly different (***, p<0.001) based on a contingency test. (I,J) qPCR analysis of pro-inflammatory genes. RNA samples from infected embryos (St Ra) and their controls were taken at 5 dpi to determine differences between *myd88*$^{-/-}$ (Mu) and wild type (Wt) in the expression levels of *il1b* (I) and *mmp9* (J). Each data point represents an individual embryo and lines indicate the mean relative expression level, with uninfected wild type set at 1. Statistical analysis performed by one-way ANOVA with Tukey's Multiple Comparison method as a post-hoc test. The mean expression levels of both genes were lower in infected mutants than in infected wild types, but the difference for *il1b* was not significant (ns) while the difference for mmp9 was significant with p<0.001 (***).

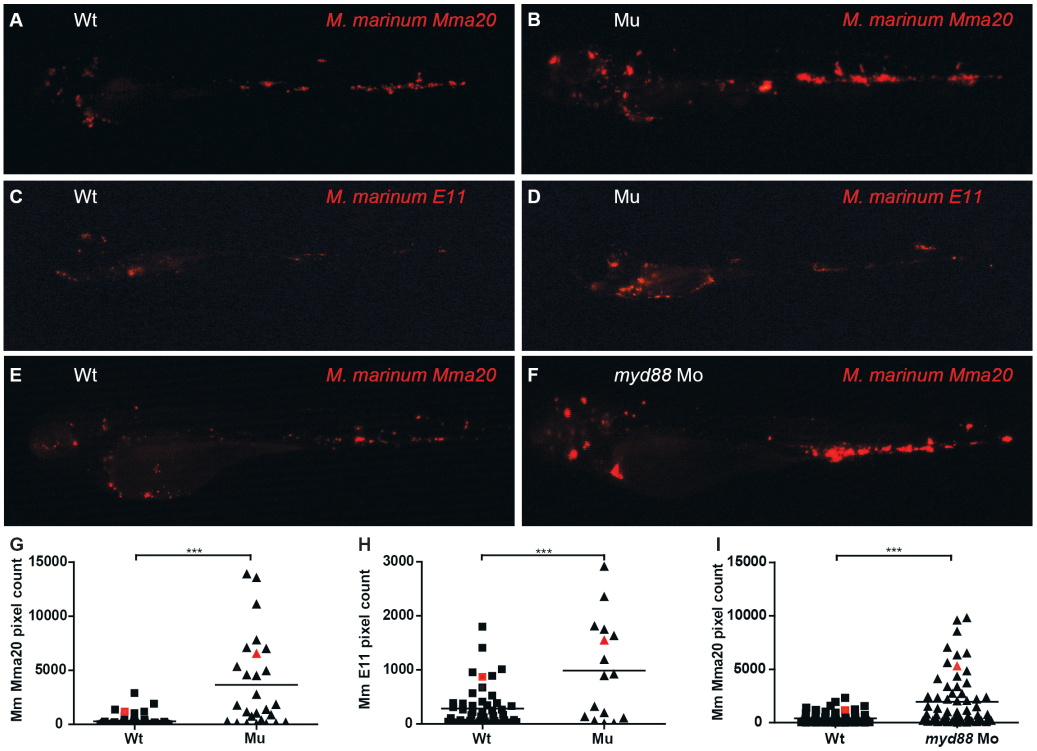

Figure 6: Bacterial burdens of *myd88*$^{-/-}$ and wild type embryos infected with *M. marinum*. (A-F) Representative stereo fluorescence images of infected embryos. At 28 hpf, *myd88*$^{-/-}$ (Mu) and wild type (Wt) embryos were infected with approximately 200 CFU of mCherry-labeled *M. marinum* strain Mma 20 (A,B) or strain E11 (C,D) by injection into the blood island and stereo fluorescence images were taken at 3 (Mma20 strain) or 5 dpi (E11 strain). For comparison, wild type and Myd88 morpholino-injected embryos were infected with the same dose of *M. marinum* Mma 20 (E,F-). (G-H) Quantification of bacterial burden. Red symbols indicate which infected individuals are shown as representative images (A-F). Bacterial pixel counts were determined based on stereo fluorescence images. Significant differences (***, $p<0.001$) were determined by one-way ANOVA with Tukey's Multiple Comparison method as a post-hoc test.

splice-morpholino against *myd88*[31]. We observed similar differences between *myd88*$^{-/-}$ and wild type embryos as for *myd88* morpholino injected embryos versus wild type (figure 6G and I). To further validate that the truncated version of Myd88 described here is inactive, we injected an AUG-morpholino targeting the *myd88* transcript in both wild type and mutant embryos[29]. The AUG-morpholino increased infection in wild type individuals compared to mismatch morpholino injected wild types, but did not increase infection in *myd88*$^{-/-}$ compared to mismatch-control injected mutants (supplementary figure 2). These results support that *myd88*^{hu3568} is a null mutant allele and demonstrate that Myd88-dependent innate immune signaling is required for the control of *M. marinum* infection in zebrafish embryos.

Myd88-signaling is required for induction of key components of the innate immune system during mycobacterial infection

Recently, the zebrafish has been successfully used to unravel the role of dysregulated Tnf levels during mycobacterial disease, showing that either too little or too much Tnf leads to aggravated infection[41,42]. We performed qPCR analysis on RNA from individual *myd88*$^{-/-}$ and wild type embryos infected with *M. marinum* Mma20 at a time point with clear granuloma formation (4 dpi). Both *il1b* and *tnfa* were expressed at significantly lower levels in infected *myd88*$^{-/-}$ embryos (figure 7A and B). Using a morpholino knockdown approach, it was previously shown that the mycobacterial virulence factor ESAT-6 can induce *mmp9* expression in host epithelial cells independent of Myd88[43]. Consistent with this result, we found that part of the host's *mmp9* induction occurred independent of Myd88 during infection with *M. marinum* (figure 7C). However, the overall level of *mmp9* expression was significantly decreased in infected *myd88*$^{-/-}$ compared to wild type embryos. Although the average expression of the chemotactic cytokines *il8* and *cxcl-c1c* was lower in infected *myd88*$^{-/-}$ compared to infected wild type, the difference was not significant (figure 7D and E). Finally, the anti-viral cytokine interferon phi1 (*ifnphi1*) was induced independently of Myd88 in both infected groups (figure 7F). In conclusion, like during *E. tarda* and *S. typhimurium* infection, Myd88-signaling is required for induction of key components of the innate immune system during mycobacterial infection.

Discussion

myd88*^{hu3568} carries a non-functional allele of *myd88

In this report we describe a zebrafish mutant for Myd88, a central component in TLR/IL1R-signaling. A premature stop codon in the mutant allele deletes the complete sequence of the domain important for interaction with TLRs (TIR domain) and disrupts the domain required for interaction with IRAKs (death domain) by truncating it before the location of a critical residue (K95) for signaling [44]. In addition to disruption of the coding sequence, *myd88* mutant mRNA was expressed at a significantly lower level than mRNA of the wild type allele. This may be explained by a lower stability of *myd88*^{hu3568} mRNA and/or by a possible feed-back mechanism by which wild type Myd88 regulates its own expression level. RT-PCR analysis of *myd88* transcripts in heterozygous individuals demonstrated that the mutant transcript indeed has a lower stability (supplementary figure 1). Innate immune responses to stimulation with known Myd88-dependent TLR ligands, LPS and flagellin, and bacterial challenge were significantly affected in *myd88* mutants. The non-functional role of the mutant allele is further supported by the fact that the phenotype of *myd88*$^{-/-}$ embryos infected with *M. marinum* is phenocopied by morpholino knockdown of *myd88* expression and that morpholino injection could not further enhance *M. marinum* infection levels in *myd88* mutants (figure 6, supplementary figure 2).

Although early leukocyte hematopoiesis was not affected in these mutants, we observed a striking increase in mortality during larval development between 8 and 20 dpf.

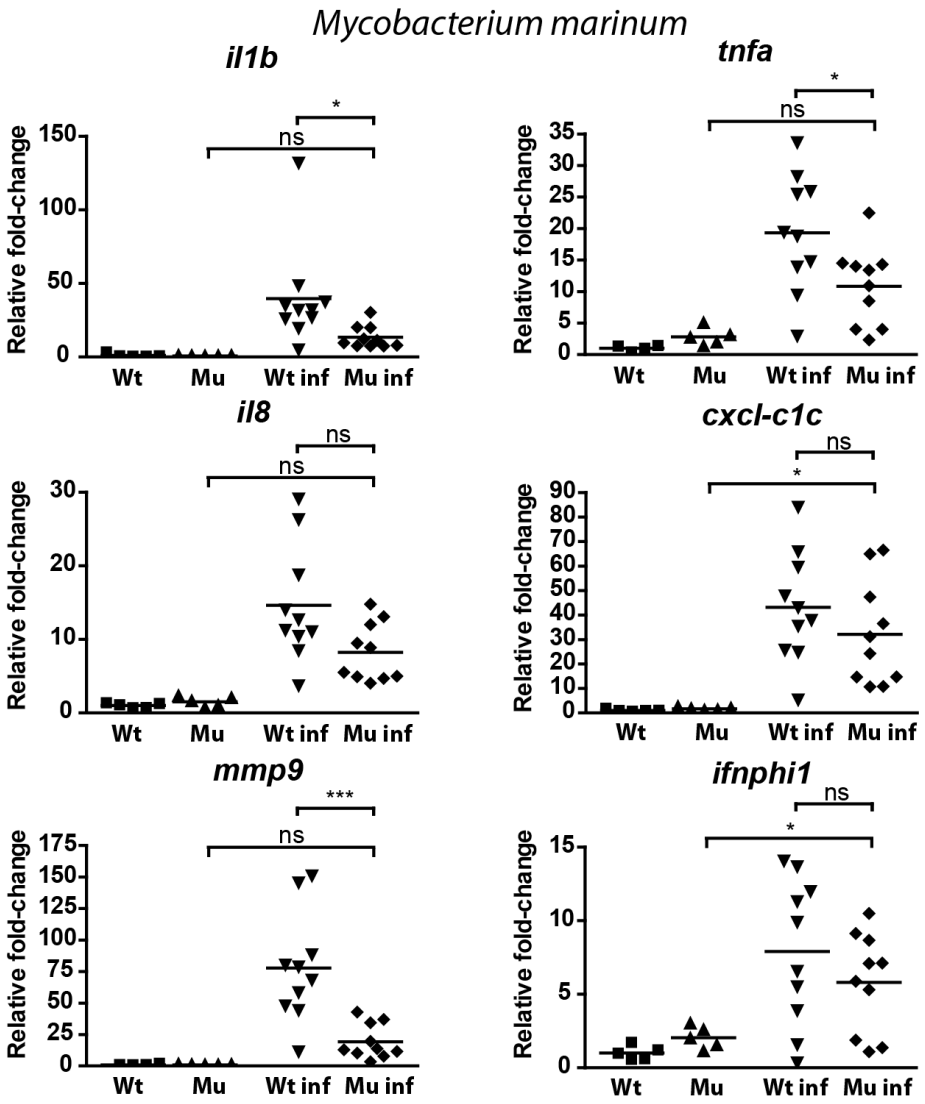

Figure 7: qPCR analysis of the response of *myd88*$^{-/-}$ and wild type embryos to *M. marinum* infection. Expression of *il1b*, *tnfa*, *il8*, *cxcl-c1c*, *mmp9*, and *ifnphi1* was analyzed by qPCR in *M. marinum* Mma20-infected wild type (Wt) and mutant (Mu) embryos. RNA samples from *M. marinum* infected embryos (inf) and uninfected controls were taken at 4 dpi. Each data point represents an individual embryo and lines indicate the mean relative expression level, with uninfected wild type set at 1. Significant differences (*,p<0.05; **, p<0.01; ***, p<0.001) were calculated by one-way ANOVA with Tukey's Multiple Comparison method as a post-hoc test.

The mortality rate of developing *myd88*$^{-/-}$ larvae decreased after this period, which might be correlated with the onset of active adaptive immunity. Nevertheless, adult *myd88*$^{-/-}$ zebrafish still display increased mortality compared to wild types. For instance, fin clipping of adult *myd88*$^{-/-}$ for genotyping purposes is followed by a higher incidence of death in the next days, possibly caused by infections associated with the wounded tailfin or by increased stress sensitivity (data not shown). This is similar to what was observed for *rag1*$^{-/-}$ zebrafish lacking functional T- and B-cells[45]. Interestingly, humans with defective MYD88 suffer from a primary immunodeficiency, with life-threatening infections occurring during early infancy[46]. Children with this deficiency have a cumulative mortality of 30-40%[46], while adult patients with this immune deficiency had no major infections[47]. This difference was ascribed to the development of proficient adaptive immune responses later in life that may compensate for the defects in the inflammatory reaction[13], a hypothesis that is supported by our observations on the survival of *myd88*$^{-/-}$ zebrafish. With its temporal separation between active innate and adaptive immunity, the *myd88*$^{-/-}$ zebrafish will be an ideal tool to further investigate this phenomenon.

***myd88*$^{-/-}$ mutant as a research model for immunity, cancer, and development**

The *myd88* mutant presented here is a valuable model to determine the role of TLR/IL1R signaling and innate immunity in numerous important processes. Not only could it be used to study host-pathogen interactions in zebrafish[21], but also to study the role of TLR signaling in the tumor microenvironment[48], as well as the role of Myd88 in the establishment of normal intestinal microbiota and maturation of the immune system during development[49]. The fact that these processes require a certain progression of larval development in order to be studied makes a mutant line more useful than a morpholino knock down approach. In this report, we used the *myd88* mutant to determine the role of TLR-Myd88 signaling during bacterial infections in zebrafish embryos and larvae. Migration of leukocytes towards bacteria[50] and phagocytosis of bacteria are not affected by the absence of Myd88 (figure 1F and 5B). Nevertheless, we found that *myd88*$^{-/-}$ embryos are more susceptible to infection by acute bacterial pathogens (*E. tarda* and *S. typhimurium*), chronic bacterial pathogens (*M. marinum* strains), and even non-pathogenic mutant bacteria (*S. typhimurium* Ra). The increased susceptibility to bacterial infections is a result of the inability of *myd88*$^{-/-}$ embryos to mount an appropriate innate immune response towards these invading microbes. Our transcriptome analysis revealed that important pro-inflammatory regulators are expressed at lower levels in infected *myd88*$^{-/-}$ embryos, including the genes encoding the components of the transcription factors NFκB and AP-1, and the cytokine Il1b (figure 3). These differences could not have been caused by variations in the injection dose, since we visually controlled for this by using fluorescently labeled bacteria. Since the embryos used for microarray analysis of gene expression were offspring from heterozygous parents, we could not exclude the possibility that maternally deposited Myd88 influenced our observations. Therefore, we validated our results using larger groups of single embryos from homozygous wild type or mutant parents, also demonstrating

that the induction levels of innate immune response genes were in significantly lower ranges in mutant than in wild type embryos (figures 5 and 8).

An important finding is that we identified genes, including the chemotactic cytokine *il8*, of which the expression was strongly dependent on Myd88-signaling during infection with one pathogen, but Myd88-independent for another pathogen. When analyzed on a larger group of *myd88*$^{-/-}$ and wild type embryos infected with *E. tarda* and *S. typhimurium*, we demonstrated that the level of *il8* expression in infected *myd88*$^{-/-}$ was lower for both pathogens, but the difference with wild type was only significant during *E. tarda* infection. The natural fish pathogen *E. tarda* may have evolved more specialized methods of manipulating or evading the immune system of their aquatic hosts, compared to the natural mammalian pathogen *S. typhimurium*. This possibility is also reflected in the total numbers of significantly up- or downregulated microarray probes during infection with these two pathogens, which was almost two-fold higher in *S. typhimurium* infection compared with *E. tarda* infection (figure 2A and B). A similar situation occurs when the transcriptome of zebrafish embryos exposed to *E. tarda* is compared to embryos exposed to *Pseudomonas aeruginosa*, a broad host range pathogen, capable of infecting plants, invertebrates, and vertebrates[37].

The *myd88*-dependency of *E. tarda* and *S. typhimurium* induced *il1b* and *mmp9* expression was consistent with our earlier observations in *myd88* morpholino knockdown studies, where the induction of these genes by *S. typhimurium* infection was also found to be *myd88*-dependent[23]. However, in the previous studies it was not possible to discriminate between complete or partial *myd88*-dependency because the morpholino knockdown effect itself may be incomplete. With the use of the mutant line we could now establish that the *E. tarda* or *S. typhimurium*-induced *il1b* expression at 8 hpi is lower but not completely absent in *myd88*$^{-/-}$ embryos, and that *mmp9* induction at this time point is completely inhibited by Myd88 deficiency during *E. tarda* infection, while partial induction occurs during *S. typhimurium* infection. Furthermore, a partial induction of *tnfa* was observed in *myd88* mutants during *M. marinum* infection, while *tnfa* induction during *S. typhimurium* infection was not affected by Myd88 deficiency. The (partial) Myd88 dependency of several interleukin and chemokine genes was in agreement with studies of cells and organs from *Myd88*-deficient mice[9, 14, 17, 51-53]. The gene for Ifnphi1*,* which belongs to the type I interferon group[54], was dependent on Myd88 for its induction during *S. typhimurium* infection, as was described for mouse *IFN1* when macrophages lacking MYD88 were stimulated with LPS[51].

Myd88-independent limitation of the growth of non-pathogenic bacteria

When *myd88*$^{-/-}$ embryos were infected with non-pathogenic *S. typhimurium* Ra bacteria, we observed large variation in *il1b* expression levels (figure 5I). Approximately half of the infected *myd88*$^{-/-}$ larvae showed *il1b* expression levels comparable to uninfected controls, while the other half displayed *il1b* expression at a similar level as infected wild types. This variation was also reflected in the outcome of infection observed by

microscopy, ranging from complete clearance of the bacteria to lethality of the embryos (figure 5H). The data clearly shows that a subset of *myd88*$^{-/-}$ embryos were capable of inducing pro-inflammatory gene expression and even clear the infection in the absence of Myd88. Potential mechanisms that could be responsible for recognizing and clearing *S. typhimurium Ra* bacteria in the absence of Tlr-Myd88 signaling are other PRRs, like NOD-like receptors or C-type lectins, or activation of the complement system. It is known that *S. typhimurium* Ra are more susceptible to complement lysis, due to a defect in the synthesis of the LPS O-antigen[55]. Transcriptome analysis of infected *myd88*$^{-/-}$ embryos revealed that expression of genes involved in complement is for a large part independent of Myd88 (figure 3). It has also been shown that complement component C5a is a potent endogenous pro-inflammatory peptide, capable of triggering production of Il1b upon infection [56]. TLRs and complement can independently induce pro-inflammatory responses, but their synergistic interaction results in amplified responses[57]. This may explain why *il1b* induction in *myd88*$^{-/-}$ embryos infected with pathogenic bacteria was significantly lower, but not completely absent (figure 4). Finally, some TLRs, like TLR4, can signal via both Myd88-dependent and –independent routes. It is possible that loss of one route can be (partially) compensated by the other route. The presence of compensatory signaling routes is also suggested by the observed gene expression following flagellin injection, which led to a completely abrogated *il1b* response in *myd88* mutant embryos, while *mmp9* induction was similar to wild type level.

Myd88-signaling has a protective role during early mycobacterial pathogenesis

Although it has been shown that the innate immune system can control early mycobacterial infections[58], the role of MYD88 in mycobacterial disease remains controversial. Mice deficient in MYD88 are more susceptible to infection by *Mycobacterium tuberculosis*[20], but it remains unclear whether this is due to the function of MYD88 in innate responses or in adaptive immunity. More recently, MYD88 polymorphisms in a Columbian population were not associated with increased susceptibility to Mycobacterium tuberculosis[59]. We used the *myd88* mutant zebrafish line to study the function of this gene during mycobacterial infection in zebrafish larvae that do not yet possess a functional adaptive immune system. We demonstrated that Myd88 is important for early control of these infections, since homozygous *myd88* mutant and Myd88 morpholino injected larvae showed accelerated formation of granulomas and at least 5-fold higher bacterial burdens compared to their wild type siblings when infected with *M. marinum* strains. Morpholino knockdown of the Tnf receptor and Mmp9 has also been shown to increase *M. marinum* granuloma formation and bacterial burden[43, 60]. In agreement, the impaired control of *M. marinum* in the absence of functional Myd88 is most likely caused by a marked reduced induction of *mmp9* and pro-inflammatory cytokines, like *il1b* and *tnfa* (figure 7). These data point towards a central role for Myd88 in innate immunity during the early stages of mycobacterial pathogenesis. Interestingly, expression of most immune related genes at the time point of granuloma formation was not completely abolished in *myd88*$^{-/-}$ embryos, demonstrating that other pathways also contribute to

attract and activate immune cells at this point. These results from application of the *myd88* mutant in a zebrafish model for tuberculosis illustrate how this mutant could serve as a valuable tool for studying innate immune responses in many other zebrafish models for human infectious diseases, inflammatory disorders, and cancer, which have been developed in recent years.

Materials and methods

Zebrafish husbandry

Zebrafish were handled in compliance with the local animal welfare regulations and maintained according to standard protocols (www.zfin.org). Embryos were grown at 28.5-30°C in egg water (60µg/ml Ocean Salts). For the duration of bacterial injections embryos were kept under anaesthesia in egg water containing 0.02% buffered 3-aminobezoic acid ethyl ester (Tricaine).

Myd88 mutant, genotyping, and morpholino injection

The *myd88*^{hu3568} mutant allele was identified by sequencing of an ENU-mutagenized zebrafish library. The mutant line was obtained from the Hubrecht Laboratory and the Sanger Institute Zefrafish Mutation Resource. Heterozygous carriers of the mutation were outcrossed twice against wild type (AB strain), and were subsequently incrossed twice. Heterozygous fish of the resulting family were used to produce embryos for the microarray and *M. marinum* infection experiments. In all other experiments, we used embryos from *myd88*$^{-/-}$/*mpx::egfp* or *myd88*$^{+/+}$/*mpx::egfp*GFP parents, obtained by incrossing the heterozygous offspring of *myd88*+/- fish outcrossed against *Tg*(*mpx*::*egfp*)^{i114} [34]. For, genotyping, genomic DNA was amplified using forward primer 5'-GAGGCGATTCCAGTAACAGC-3' and reverse primer 5'-GAAGCGAACAAAGAAAAGCAA-3' and the product of this reaction was digested with MseI. The mutant allele can be distinguished from the wild type allele by the presence of an extra MseI site that cuts a fragment of approximately 300 bp into 200 and 100 bp products. Determining the stability of the mutant transcript versus the wild type transcript was done with a RT-PCR using forward primer 5'-GAGGCGATTCCAGTAACAGC-3' and reverse primer 5'-GAAAGCATCAAAGGTCTCAGGTG-3' and the product of this reaction was digested with MseI. Knockdown of *myd88* by splice morpholino was performed as previously described[31]. Knockdown of *myd88* by AUG-morpholino was previously described by Van der Sar et al. (2006).

Immunohistochemistry

Immunolabeling with L-plastin antibody[61] and Alexa568-conjugated secondary antibody was as described[62].

Injection conditions

Edwardsiella tarda strain FL6-60 labeled with mCherry[63]; *Salmonella typhimurium* wild type strain SL1027 and its isogenic LPS derivative SF1592 (Ra), both containing the DsRed expression vector pGMDs3[23]; and *Mycobacterium marinum* strains Mma20

and E11 labeled with mCherry[64] were used for the infection of zebrafish embryos. Bacteria were washed and subsequently suspended in PBS (phosphate-buffered saline), amended with 2% polyvinylpyrrolidone (PVP) for *E. tarda* and *M. marinum*. Embryos were manually dechorionated at 24 hpf. Approximately 150-200 CFUs were injected into the blood island after the onset of blood flow at 28 hpf, or PBS (2% PVP for *E. tarda* and *M. marinum*) was injected as a control. After injection, embryos were kept at 28°C. Purified TLR ligands: LPS from *S. enterica* serovar *typhimurium* (Sigma, #L6511), poly I:C high molecular weight (Invivogen, #tirl-pic), flagellin from *S. enterica* serovar *typhimurium* (Invivogen, #fla-st ultrapure).

Phagocytosis assay

E. coli pHrodo particles (**Life Technologies Europe BV, Bleijswijk, Netherlands**) were injected into the blood island at 28 hpf (1nl of a 0.5 mg/ml solution). Fluorescent pixel quantification was performed at 2 hpi.

DNA and RNA isolation

The single embryo RNA isolation procedure using TRI reagent (**Life Technologies Europe BV, Bleijswijk, the Netherlands**) was performed as previously described by De Jong et al[65]. DNA for genotyping was isolated from the organic phase and was done according to the alternate DNA isolation protocol of the TRI reagent DNA/protein isolation protocol, using glycogen as a co-precipitant. RNA from the aqueous phase was purified using the Rneasy MinElute Cleanup kit (QIAGEN Benelux B.V., Venlo, Netherlands).

Microarray analysis

Microarray was performed using our custom-designed Agilent 44k platform GPL10042, as previously described[37]. The raw data were submitted to the Gene Expression Omnibus database under accession no. GSE39274. To compare wild type control, mutant control, wild type infected and mutant infected samples, a re-ratio experiment was performed using the Rosetta built-in re-ratio with common reference application. Data were analyzed at the level of probes with significant cut-offs for the ratios set at 2-fold change at $p<10^{-5}$. For the heat map construction the fold change values of significant probes representing the same gene were averaged. Gene ontology (GO) analysis was performed using the GeneTools eGOn v2.0 web-based gene ontology analysis software[66].

cDNA synthesis and quantitative reverse transcriptase PCR

cDNA synthesis reactions and qPCR were performed as previously described and normalized against the expression of *ppial* as a housekeeping gene[37]. Sequences for forward and reverse primers are described in supplementary table 1.

Microscopy and fluorescent pixel quantification

Embryos injected with fluorescently labeled bacteria or pHrodo-labeled *E. coli* cell wall particles were imaged using a (Leica MZ16FA stereo fluorescence microscope with Leica DFC420C camera. Total fluorescent pixels per fish were determined using dedicated software[67].

Acknowledgements

We thank Ulrike Nehrdich, Laura van Hulst, and Davy de Witt for fish care and Phil Elks for critically reading the manuscript. For providing the zebrafish mutant allele *myd88*^{hu3568} we thank the Hubrecht Laboratory and the Sanger Institute Zebrafish Mutation Resource (ZF-MODELS Integrated Project; contract number LSHG-CT-2003-503496; funded by the European Commission), also sponsored by the Welcome Trust; grant number WT 077047/Z/05/Z). This work was further supported by the Smart Mix Program of the Netherlands Ministry of Economic Affairs and the Ministry of Education, Culture and Science, the European Commission 6th Framework Project ZF-TOOLS (LSHG-CT-2006-037220) and the European Commission 7th framework project ZF-HEALTH (HEALTH-F4-2010-242048).

Competing interests statement

The authors have nothing to declare.

Author contributions

All authors conceived and designed the experiments. MV and JS performed the experiments and analyzed the data under supervision of AM. MV wrote the manuscript and the final version was read and approved by all authors.

Translational impact box

Background

Toll-like receptors (TLRs) are an important class of receptors that can detect microbial and danger signals during infection and inflammation. As an adaptor molecule, myeloid differentiation factor 88 (MYD88) is central in TLR-signaling and innate immunity, which is illustrated by the fact that patients with MYD88 deficiency suffer from a primary immunodeficiency syndrome. The use of zebrafish as a model for infectious diseases, inflammatory disorders, cancer, and other immune related disease is growing rapidly, owing to many advantages for intravital imaging, genetic screening, and high-throughput drug discovery. Therefore, zebrafish mutants for important components of the immune system are eagerly awaited.

Results

In this study, we have characterized a zebrafish line with a premature stopcodon in the *myd88* gene, which is the first zebrafish mutant for a TLR/IL1R-signaling component. The mutant line appeared to be immune-compromised and had a higher susceptibility to infection by acute (*Edwardsiella tarda* and *Salmonella typhimurium*) and chronic (*Mycobacterium marinum*) bacterial pathogens. Microarray and quantitative PCR (qPCR) analysis of gene expression revealed that expression of transcription factors central to

innate immunity, like NFκB and AP-1, and pro-inflammatory genes like *il1b* and *mmp9* are dependent on Myd88-signaling during these bacterial infections. Nevertheless, expression of immune genes independent of Myd88 in these mutants was sufficient to limit bacterial burdens of an attenuated *S. typhimurium* strain.

Implications and future directions

The zebrafish *myd88* mutant is a valuable addition to mammalian knockout models, especially when combined with transgenic lines with fluorescently marked immune cells that facilitate intravital imaging. During zebrafish development, innate immunity is active from day 1 onwards, whereas adaptive immunity is not fully functional during the first weeks. Zebrafish mutant models therefore can be used not only to study the interplay between innate and adaptive immunity (at juvenile and adult stages), but also provide the possibility to study functions of the innate immune system with minimal interference of adaptive immunity (at embryo and larval stages). In our study we exploited this possibility using a zebrafish model for tuberculosis and demonstrated that Myd88 has a protective role during early mycobacterial pathogenesis in zebrafish larvae when only innate immunity is functional. The zebrafish *myd88* mutant model will also be a valuable tool for studying innate immune responses in many other zebrafish models for human infectious diseases that have emerged in the recent years. Furthermore, it can make an important contribution to zebrafish models for inflammatory disorders and cancer.

References

1. Medzhitov, R. & Janeway, C., Jr. Innate immune recognition: mechanisms and pathways. *Immunol Rev* **173**, 89-97 (2000).
2. Matzinger, P. The danger model: a renewed sense of self. *Science* **296**, 301-305 (2002).
3. Takeda, K. & Akira, S. Microbial recognition by Toll-like receptors. *J Dermatol Sci* **34**, 73-82 (2004).
4. Gay, N.J., Gangloff, M. & O'Neill, L.A. What the Myddosome structure tells us about the initiation of innate immunity. *Trends Immunol* **32**, 104-109 (2011).
5. Lin, S.C., Lo, Y.C. & Wu, H. Helical assembly in the MyD88-IRAK4-IRAK2 complex in TLR/IL-1R signalling. *Nature* **465**, 885-890 (2010).
6. Burns, K. *et al.* MyD88, an adapter protein involved in interleukin-1 signaling. *J Biol Chem* **273**, 12203-12209 (1998).
7. Muzio, M., Ni, J., Feng, P. & Dixit, V.M. IRAK (Pelle) family member IRAK-2 and MyD88 as proximal mediators of IL-1 signaling. *Science* **278**, 1612-1615 (1997).
8. Wesche, H., Henzel, W.J., Shillinglaw, W., Li, S. & Cao, Z. MyD88: an adapter that recruits IRAK to the IL-1 receptor complex. *Immunity* **7**, 837-847 (1997).
9. Adachi, O. *et al.* Targeted disruption of the MyD88 gene results in loss of IL-1- and IL-18-mediated function. *Immunity.* **9**, 143-150 (1998).
10. Sun, D. & Ding, A. MyD88-mediated stabilization of interferon-gamma-induced cytokine and chemokine mRNA. *Nat Immunol* **7**, 375-381 (2006).

11. von Bernuth, H. *et al.* Pyogenic bacterial infections in humans with MyD88 deficiency. *Science* **321**, 691-696 (2008).

12. Picard, C. *et al.* Clinical features and outcome of patients with IRAK-4 and MyD88 deficiency. *Medicine (Baltimore)* **89**, 403-425 (2010).

13. Netea, M.G., Wijmenga, C. & O'Neill, L.A. Genetic variation in Toll-like receptors and disease susceptibility. *Nat Immunol* **13**, 535-542 (2012).

14. Kawai, T., Adachi, O., Ogawa, T., Takeda, K. & Akira, S. Unresponsiveness of MyD88-deficient mice to endotoxin. *Immunity.* **11**, 115-122 (1999).

15. Akira, S. & Takeda, K. Functions of toll-like receptors: lessons from KO mice. *C R Biol* **327**, 581-589 (2004).

16. Scanga, C.A. *et al.* Cutting edge: MyD88 is required for resistance to Toxoplasma gondii infection and regulates parasite-induced IL-12 production by dendritic cells. *J Immunol* **168**, 5997-6001 (2002).

17. Takeuchi, O., Hoshino, K. & Akira, S. Cutting edge: TLR2-deficient and MyD88-deficient mice are highly susceptible to Staphylococcus aureus infection. *J.Immunol.* **165**, 5392-5396 (2000).

18. Edelson, B.T. & Unanue, E.R. MyD88-dependent but Toll-like receptor 2-independent innate immunity to Listeria: no role for either in macrophage listericidal activity. *J.Immunol.* **169**, 3869-3875 (2002).

19. Naiki, Y. *et al.* MyD88 is pivotal for the early inflammatory response and subsequent bacterial clearance and survival in a mouse model of Chlamydia pneumoniae pneumonia. *J Biol Chem* **280**, 29242-29249 (2005).

20. Ryffel, B. *et al.* Innate immunity to mycobacterial infection in mice: critical role for toll-like receptors. *Tuberculosis (Edinb)* **85**, 395-405 (2005).

21. Meijer, A.H. & Spaink, H.P. Host-pathogen interactions made transparent with the zebrafish model. *Curr Drug Targets* **12**, 1000-1017 (2011).

22. Herbomel, P., Thisse, B. & Thisse, C. Ontogeny and behaviour of early macrophages in the zebrafish embryo. *Development* **126**, 3735-3745 (1999).

23. Stockhammer, O.W., Zakrzewska, A., Hegedus, Z., Spaink, H.P. & Meijer, A.H. Transcriptome profiling and functional analyses of the zebrafish embryonic innate immune response to Salmonella infection. *J Immunol* **182**, 5641-5653 (2009).

24. van der Vaart, M., Spaink, H.P. & Meijer, A.H. Pathogen recognition and activation of the innate immune response in zebrafish. *Adv Hematol* **2012**, 159807 (2011).

25. Hall, C. *et al.* Transgenic zebrafish reporter lines reveal conserved Toll-like receptor signaling potential in embryonic myeloid leukocytes and adult immune cell lineages. *J Leukoc Biol* **85**, 751-765 (2009).

26. Lam, S.H., Chua, H.L., Gong, Z., Lam, T.J. & Sin, Y.M. Development and maturation of the immune system in zebrafish, Danio rerio: a gene expression profiling, in situ hybridization and immunological study. *Dev.Comp Immunol.* **28**, 9-28 (2004).

27. Mione, M., Meijer, A.H., Snaar-Jagalska, B.E., Spaink, H.P. & Trede, N.S. Disease modeling in zebrafish: cancer and immune responses--a report on a workshop held in Spoleto, Italy, July 20-22, 2009. *Zebrafish* **6**, 445-451 (2009).

28. Bedell, V.M., Westcot, S.E. & Ekker, S.C. Lessons from morpholino-based screening in zebrafish. *Brief Funct Genomics* **10**, 181-188 (2011).

29. Van der Sar, A.M. *et al.* MyD88 innate immune function in a zebrafish embryo infection model. *Infection and Immunity* **74**, 2436-2441 (2006).

30. Liu, M., John, C.M. & Jarvis, G.A. Phosphoryl moieties of lipid A from Neisseria meningitidis and N. gonorrhoeae lipooligosaccharides play an important role in activation of both MyD88- and TRIF-dependent TLR4-MD-2 signaling pathways. *J Immunol* **185**, 6974-6984 (2010).

31. Bates, J.M., Akerlund, J., Mittge, E. & Guillemin, K. Intestinal alkaline phosphatase detoxifies lipopolysaccharide and prevents inflammation in zebrafish in response to the gut microbiota. *Cell Host Microbe* **2**, 371-382 (2007).

32. Cheesman, S.E., Neal, J.T., Mittge, E., Seredick, B.M. & Guillemin, K. Epithelial cell proliferation in the developing zebrafish intestine is regulated by the Wnt pathway and microbial signaling via Myd88. *Proc Natl Acad Sci U S A* **108 Suppl 1**, 4570-4577 (2010).

33. Oehlers, S.H. *et al.* A chemical enterocolitis model in zebrafish larvae that is dependent on microbiota and responsive to pharmacological agents. *Dev Dyn* **240**, 288-298 (2011).

34. Renshaw, S.A. *et al.* A transgenic zebrafish model of neutrophilic inflammation. *Blood* (2006).

35. Sullivan, C. *et al.* The gene history of zebrafish tlr4a and tlr4b is predictive of their divergent functions. *J Immunol* **183**, 5896-5908 (2009).

36. Sepulcre, M.P. *et al.* Evolution of lipopolysaccharide (LPS) recognition and signaling: fish TLR4 does not recognize LPS and negatively regulates NF-kappaB activation. *J Immunol* **182**, 1836-1845 (2009).

37. van Soest, J.J. *et al.* Comparison of static immersion and intravenous injection systems for exposure of zebrafish embryos to the natural pathogen Edwardsiella tarda. *BMC Immunol* **12**, 58 (2011).

38. Van der Sar, A.M. *et al.* Zebrafish embryos as a model host for the real time analysis of Salmonella typhimurium infections. *Cell.Microbiol.* **in press** (2003).

39. Hsu, K. *et al.* The pu.1 promoter drives myeloid gene expression in zebrafish. *Blood* **104**, 1291-1297 (2004).

40. Davis, J.M. *et al.* Real-time visualization of mycobacterium-macrophage interactions leading to initiation of granuloma formation in zebrafish embryos. *Immunity* **17**, 693-702 (2002).

41. Tobin, D.M. *et al.* The lta4h locus modulates susceptibility to mycobacterial infection in zebrafish and humans. *Cell* **140**, 717-730 (2010).

42. Tobin, D.M. *et al.* Host genotype-specific therapies can optimize the inflammatory response to mycobacterial infections. *Cell* **148**, 434-446 (2012).

43. Volkman, H.E. *et al.* Tuberculous granuloma induction via interaction of a bacterial secreted protein with host epithelium. *Science* **327**, 466-469 (2010).

44. Loiarro, M. *et al.* Identification of critical residues of the MyD88 death domain involved in the recruitment of downstream kinases. *J Biol Chem* **284**, 28093-28103 (2009).

45. Jima, D.D. *et al.* Enhanced transcription of complement and coagulation genes in the absence of adaptive immunity. *Mol Immunol* **46**, 1505-1516 (2009).

46. Ku, C.L. *et al.* Selective predisposition to bacterial infections in IRAK-4-deficient children: IRAK-4-dependent TLRs are otherwise redundant in protective immunity. *J Exp Med* **204**, 2407-2422 (2007).

47. Bousfiha, A. *et al.* Primary immunodeficiencies of protective immunity to primary infections. *Clin Immunol* **135**, 204-209 (2010).

48. Sato, Y., Goto, Y., Narita, N. & Hoon, D.S. Cancer Cells Expressing Toll-like Receptors and the Tumor Microenvironment. *Cancer Microenviron* **2 Suppl 1**, 205-214 (2009).

49. Frantz, A.L. *et al.* Targeted deletion of MyD88 in intestinal epithelial cells results in compromised antibacterial immunity associated with downregulation of polymeric immunoglobulin receptor, mucin-2, and antibacterial peptides. *Mucosal Immunol* **5**, 501-512 (2012).

50. Deng, Q., Harvie, E.A. & Huttenlocher, A. Distinct signaling mechanisms mediate neutrophil attraction to bacterial infection and tissue injury. *Cell Microbiol* (2012).

51. Hirotani, T. *et al.* Regulation of lipopolysaccharide-inducible genes by MyD88 and Toll/IL-1 domain containing adaptor inducing IFN-beta. *Biochem Biophys Res Commun* **328**, 383-392 (2005).

52. Kissner, T.L., Cisney, E.D., Ulrich, R.G., Fernandez, S. & Saikh, K.U. Staphylococcal enterotoxin A induction of pro-inflammatory cytokines and lethality in mice is primarily dependent on MyD88. *Immunology* **130**, 516-526 (2010).

53. Weighardt, H. *et al.* Organ-specific role of MyD88 for gene regulation during polymicrobial peritonitis. *Infect Immun* **74**, 3618-3632 (2006).

54. Hamming, O.J., Lutfalla, G., Levraud, J.P. & Hartmann, R. Crystal structure of Zebrafish interferons I and II reveals conservation of type I interferon structure in vertebrates. *J Virol* **85**, 8181-8187 (2011).

55. Tsolis, R.M., Adams, L.G., Ficht, T.A. & Baumler, A.J. Contribution of Salmonella typhimurium virulence factors to diarrheal disease in calves. *Infect Immun* **67**, 4879-4885 (1999).

56. Montz, H., Koch, K.C., Zierz, R. & Gotze, O. The role of C5a in interleukin-6 production induced by lipopolysaccharide or interleukin-1. *Immunology* **74**, 373-379 (1991).

57. Holst, B., Raby, A.C., Hall, J.E. & Labeta, M.O. Complement takes its Toll: an inflammatory crosstalk between Toll-like receptors and the receptors for the complement anaphylatoxin C5a. *Anaesthesia* **67**, 60-64 (2012).

58. Lesley, R. & Ramakrishnan, L. Insights into early mycobacterial pathogenesis from the zebrafish. *Curr.Opin.Microbiol.* **11**, 277-283 (2008).

59. Sanchez, D., Lefebvre, C., Rioux, J., Garcia, L.F. & Barrera, L.F. Evaluation of Toll-like receptor and adaptor molecule polymorphisms for susceptibility to tuberculosis in a Colombian population. *Int J Immunogenet* **39**, 216-223 (2012).

60. Clay, H., Volkman, H.E. & Ramakrishnan, L. Tumor necrosis factor signaling mediates resistance to mycobacteria by inhibiting bacterial growth and macrophage death. *Immunity* **29**, 283-294 (2008).

61. Mathias, J.R. *et al.* Characterization of zebrafish larval inflammatory macrophages. *Dev Comp Immunol* **33**, 1212-1217 (2009).

62. Cui, C. *et al.* Infectious disease modeling and innate immune function in zebrafish embryos. *Methods Cell Biol* **105**, 273-308 (2011).

63. Lagendijk, E.L., Validov, S., Lamers, G.E., de Weert, S. & Bloemberg, G.V. Genetic tools for tagging Gram-negative bacteria with mCherry for visualization in vitro and in natural habitats, biofilm and pathogenicity studies. *FEMS Microbiol Lett* **305**, 81-90 (2010).

64. Van der Sar, A.M. *et al.* Mycobacterium marinum strains can be divided into two distinct types based on genetic diversity and virulence. *Infection and Immunity* **72**, 6306-6312 (2004).

65. de Jong, M. *et al.* RNA isolation method for single embryo transcriptome analysis in zebrafish. *BMC Res Notes* **3**, 73 (2010).

66. Beisvag, V. *et al.* GeneTools--application for functional annotation and statistical hypothesis testing. *BMC Bioinformatics* **7**, 470 (2006).

67. Stoop, E.J. *et al.* Zebrafish embryo screen for mycobacterial genes involved in the initiation of granuloma formation reveals a newly identified ESX-1 component. *Dis Model Mech* **4**, 526-536 (2011).